DESIGN AND FABRICATION OF WIDEBAND ARCHIMEDEAN SPIRAL ANTENNA BASED ULTRA-LOW COST "GREEN" MODULES FOR RFID SENSING AND WIRELESS APPLICATIONS

Y. Amin[*], Q. Chen, L. R. Zheng, and H. Tenhunen

iPack VINN Excellence Center, Royal Institute of Technology (KTH), Stockholm, SE-16440, Sweden

Abstract—A parametric analysis is performed for a wideband Archimedean spiral antenna in recognition of an emerging concept to integrate RFID along with several applications by using a single antenna. The antenna is fabricated using state-of-the-art inkjet printing technology on various commercially available paper substrates to provide the low-cost, flexible RF modules for the next generation of "green" electronics. The effects on electromagnetic characteristics of the planar Archimedean spiral antenna, due to the use of paper are investigated besides other parameters. The proposed antenna is evaluated and optimized for operational range from 0.8–3.0 GHz. It exhibits exceptional coverage throughout numerous RFID ISM bands so do for other wireless applications.

1. INTRODUCTION

RFID (Radio Frequency Identification) is considered an emerging leading technology in future telecommunications [1, 2], automatic identification and data capture (AIDC) industries [3]. The RFID market has grown in a two-dimensional trend one side constitutes standalone RFID systems which are commonly found at present [4–6]. On the other hand, more ultramodern approach is paving its way, in which RFID needs to be integrated with broad operational array of distinct applications [7, 8] for performing different functions including navigation, broadcasting, and personal communication [9–11], to mention a few. Using different antennas to include all communication

bands is a straightforward approach, but at the same time, it leads to increasing cost, weight, more surface area for installation, and above all electromagnetic compatibility issues [12]. Thus, there is the need for wide-bandwidth antennas [13, 14]. The espousal of a single, small-sized wideband antenna is certainly more attractive because RFID is replacing other identification methods by whistling about cost-effective more efficient solutions [15, 16].

Spirals are extensively used circularly polarized wideband antennas [17]. The wideband features of spiral antenna brought it to the limelight in recent literature, particularly for miniaturization. The fundamental inspiration for miniaturization is to slow down the wave traveling within the antenna structure. Numerous approaches have been pursued to achieve it, which includes dielectric or magneto-dielectric loading, artificial materials, spiral arm shaping, distributed reactive loading and arm orienting vertically [12]. Conversely, when using the popular dielectric loading approach, the input impedance is also lowered. On the other hand, when the wave velocity is reduced by meandering of metalized arms, the axial ratio also deteriorates [17]. It has been established that coiling of the spiral arms provides for impedance control [12, 18]. The vast majority of circuits fabricated on PCB use FR-4 [19–22]; thus this volumetric design or miniaturization is weighty, whereas PET is commonly found in RFID inlays and tags. Furthermore, both FR-4, which is a ceramic-based material [23], and polyethylene terepthalate (PET) are nonbiodegradable substances that may take decades to decompose in landfills largely contributing to the bulk of annually generated electronic waste.

This paper presents parametric analysis of a flexible, wideband Archimedean antenna, which is fabricated by utilizing an exceptionally efficient and low-cost inkjet printing technique to print "green" conformal electronic circuits on paper substrate. Paper is extremely eco-friendly requiring a few months to decompose organically in landfills. Organic materials do tend to be more lossy at higher frequencies, due to their affinity to water. However, by using the correct paper type and printing process, adequate radio frequency performance is achieved on paper-based RF circuit designs. We demonstrate the successful use of the proposed inkjet printed antenna for operational range from 0.8–3.0 GHz. The design and simulations are performed using ANSYS HFSS^{TM}, whereas; the measurements are performed in an anechoic chamber dedicated to antenna characterization. The proposed antenna successfully operates throughout the operational range of interest, thus expanding the scope of simultaneously integrating several wireless modules while developing eco-friendly industrial solutions.

2. "GREEN" ANTENNAS EVOLUTION

The innovative concept of "green" broadband antennas perpetuated new set of parameters that constitute the proposed design stages mentioned in Figure 1. In contrast to traditional design flow, each stage of "green" evolution is loaded with a unique matrix of factors which need to be evaluated for integration with electronic devices. It is evident from the proposed evolution stages that the degree of
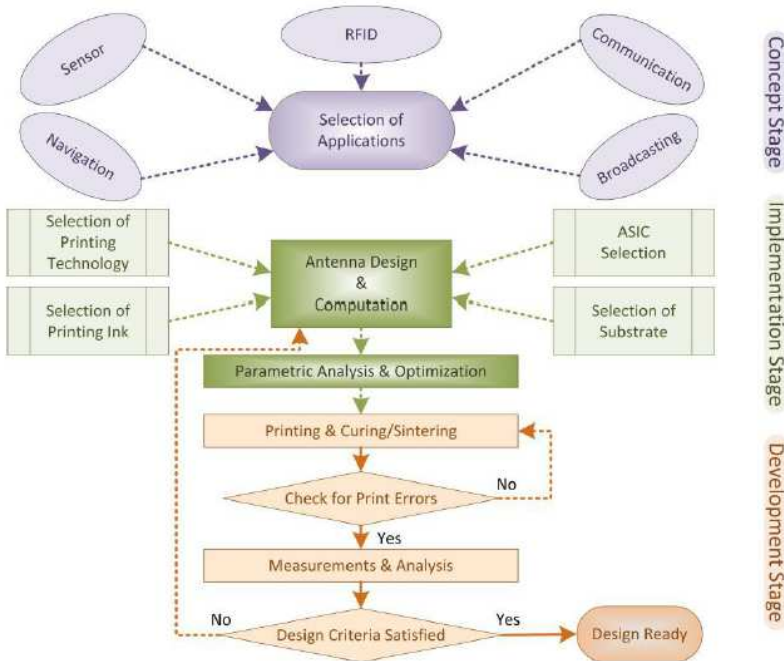

Figure 1. Evolution process of "Green" antennas for multi-module applications.

Table 1. Characterized/evaluated substrate parameters.

Substrate	Thickness (μm)	Permittivity (ε_r)	Loss Tangent
Kodak U-P Photopaper	250	3.3 (average)	0.077 (1 GHz@25°C)
HP Adv. Photopaper	250	3.3 (average)	0.04 (1 GHz@25°C)
Felix Schoeller Paper (p_e:smart)	250	3.2 (average)	0.077 (1 GHz@25°C)

freedom at the concept level, limits the choices at the implementation phase than development. Therefore, much effort is devoted to the implementation stage and design parameters are investigated and optimized categorically. Two types of conductive inks, CCI-300 from Cabot Corp. and Nano-AG-120I from Xerox Corp. are evaluated by trial printing in combination with three different types of commercially available paper substrates mentioned in Table 1. The key concept encapsulating the entire adaptation process is to achieve robust broadband antennas, which must show less sensitivity to the environmental variations that affect the paper dielectric constant.

3. SYNTHESIS OF THE ANTENNA TOPOLOGY

In order to achieve stable broadband multimode feature [24] multimode feature in far and near fields planar Archimedean spiral antenna structure is realized. Three designs of a two-arm Archimedean spiral antenna are assessed. The in-depth research proves that the Archimedean spiral is not a frequency-independent antenna structure because the spacing between the arms is specified by a constant, not an angle [25]. However, this is a contentious point because fundamentally frequency-independent performance is achieved over 10 : 1 bandwidths. The following numerical calculations are exploited to construct the proposed antenna structure in Figure 2. The centerline of the proposed Archimedean antenna is defined by:

$$r = a\phi = r_0 + (E)\phi^{(1/S)} \tag{1}$$

where,

$$a = \frac{1}{K}\frac{dK}{dC} \tag{2}$$

and C is the angle of rotation which depends on K. If the antenna is to be scaled to a frequency that is K times lower than the original
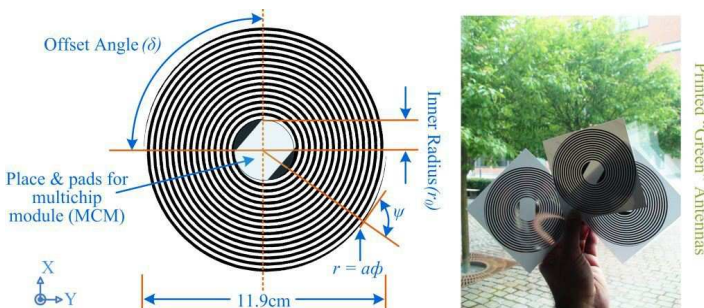

Figure 2. Dimensions & "green" theme of proposed antennas.

frequency, the antenna's physical surface must be made K times greater to maintain the same electrical dimensions [26]. The Expansion coefficient (E) and the Spiral coefficient (S) of the proposed antenna are 1 whereas, r_0 is the inner radius which is 1.6 cm. The pitch angle ψ varies with radius as:

$$\tan \psi = \frac{r}{a} \tag{3}$$

When r is large, then the pitch angle approaches $90°$. An equivalent design ratio τ_{eq}, which varies with radius, may be defined for the Archimedean spiral that has the same pitch angle ψ at radius r. Therefore,

$$\tau_{eq}(r) = e^{-2\pi/|\tan \psi|} = e^{-2\pi|a/r|} \tag{4}$$

It is worth noting here that τ_{eq} approaches 1 for large value of r. The sides of a strip may be defined in terms of the rotation angle ϕ of Figure 2 and the angle δ (offset angle is $90°$ of the proposed structure) to get:

$$r = a \left(\phi \pm \frac{\delta}{2} \right) \tag{5}$$

The radial width of the antenna strip W_r is a constant, which is independent of radius and is obtained by:

$$W_r = a\delta \tag{6}$$

The actual width of the antenna strip varies to some extent with radius and is calculated by:

$$W = a\delta \sin \psi \tag{7}$$

The spacing S_r between the centerlines of the adjacent turns for one arm is specified by:

$$S_r = 2\pi a \tag{8}$$

Furthermore, the actual spacing is given by:

$$S = S_r \sin \psi = 2\pi a \sin \psi \tag{9}$$

The two-arm spiral antenna proposed in Figure 2 for frequency band 0.8–3 GHz is self complementary when $W/S = 1/4$ or $\delta = \pi/2$ [26]. Given that the strip widths and spacings are defined by constants rather than by angles, Archimedean spiral antenna does not conform to either the frequency-independent or log-periodic principles [25]. Thus, this antenna gives autonomy to those ASIC manufacturers [27, 28] which have frequency dependent modules. In practice, it is observed that frequency independent characteristics are obtained if τ is large enough in the active region (i.e., radiation region), wherein the circumference of the radiation ring is about one

length. Alas, diminutive information has been published [12, 29] on the degradation of gain and patterns versus τ. Some published results indicate the loosely wound log-spiral performs as well as the tightly wound Archimedean spirals; however, this analysis is out of scope of this article.

4. MANUFACTURING PARAMETRIC ANALYSIS

4.1. Skin Depth Effect and Antenna Performance

It is well established that the thickness of the printed design needs to be larger or closer to the value of skin depth in order to achieve optimal performance [3, 30]. For a normal conductor, the skin depth can be computed as [31]:

$$\delta = \sqrt{\frac{1}{\pi f \mu \sigma}} \tag{10}$$

where f is the frequency, σ the conductivity, and μ the permeability of the conducting material. The conductivity of the printed traces of silver nano-particle based inks used in this research, after curing, is high enough (for Xerox ink $\approx 0.7 \times 10^7$ S/m and for Cabot ink $\approx 0.9 \times 10^7$ S/m) to be considered as a good conductor, but not as high as bulk silver. The skin depth for traces of the proposed antenna with operational frequency at 800 MHz is evaluated using Equation (10). The thickness of the printed single layer of ink from the printer used is around 200 nm (Nano-AG-120I)–600 nm (CCI-300). It has been found after careful iterations that at least three layers of printing by Cabot ink and four layers of printing by Xerox ink, are sufficient to achieve better performance under the limits imposed by various design factors.

From Figures 3(e) & (f), it is obvious that the proposed antenna with 7.5-turns has improved LHCP (Figure 3(e)) and RHCP (Figure 3(f)) gain, than antennas with 6.5-turns (Figures 3(a) & (b)), and 7-turns (Figures 3(c) & (d)). This performance criterion is achieved without enlarging the antenna's physical aperture. Specifically, the antenna with 7.5-turns at approximately 1.9 GHz exhibits a 4.7-dB, 4.5-dB and 4.4-dB gain on Kodak, HP and Felix Schoeller paper(p_e:smart) respectively, by printing with Cabot ink. Whereas, by printing with Xerox ink the gain achieved at 1.9 GHz is 4.7-dB, 4.6-dB and 4.6-dB on Kodak, HP and Felix Schoeller paper respectively. It is depicted from Figure 3 that by further increasing the number of spiral turns, the gain improves at lower frequencies. It is observed that the antenna impedance also decreases with the increase in number of turns.
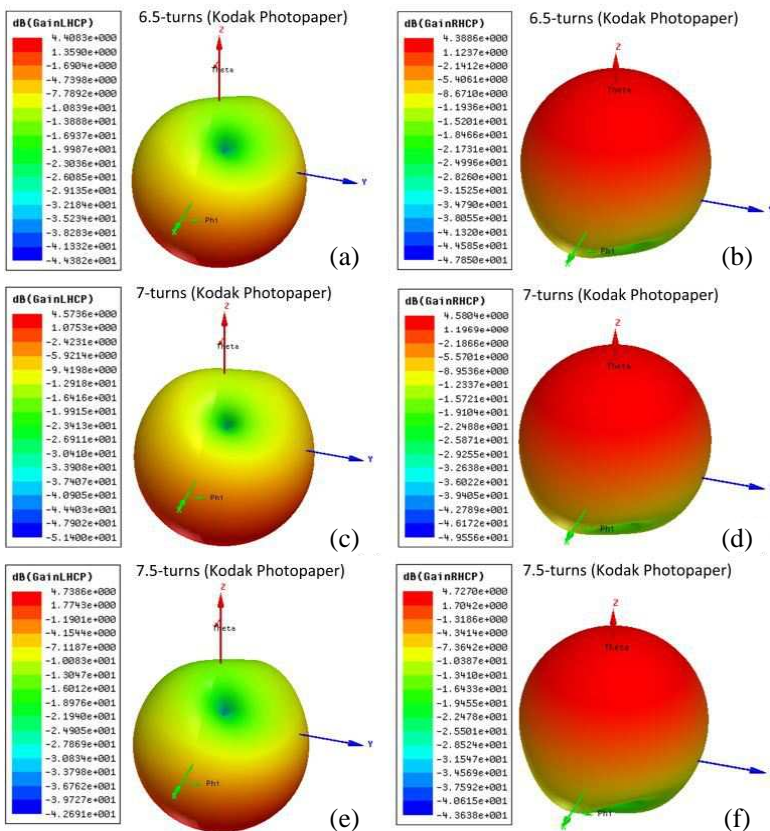
Figure 3. Simulated 3D LHCP & RHCP gain radiation patterns of antennas with 6.5, 7 and 7.5-turns.

On the other hand if the number of turns are reduced, the gain of the antenna decreases to a value which violates the design requirements because these tags are proposed for large items level tacking and information gathering. So it is mandatory for the antenna to exhibit better gain to achieve higher read range while at the same time providing readability in the near field region. Moreover, due to the consumption of expensive conductive ink, the size of the antenna has to be within economical limits for its possible realization on industrial scale. Therefore, the optimal design pattern is achieved while considering the size limits along with other performance factors for attaching to large items in the working range from 0.8–3.0 GHz is realized with 7.5-turns, and its current distribution plot is shown in Figure 4.
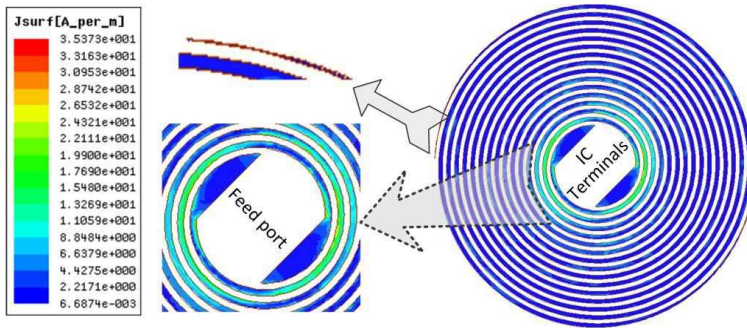
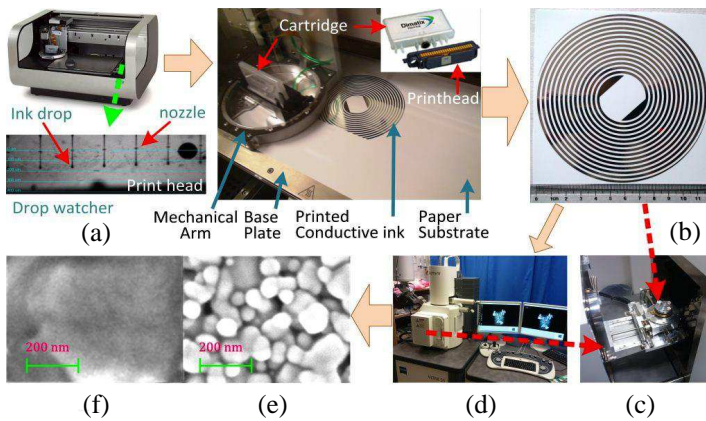**Figure 4.** The current distribution of proposed antenna at 1.9 GHz.

Figure 5. (a) Inkjet printing setup, (b) inkjet printed antenna on Felix Schoeller paper, (c) SEM sample holder, (d) ULTRA-55 FESEM Carl Zeiss setup; SEM images of three layers of printed silver nanoparticle ink, after curing 2 hr at: (e) 100°C, (f) 150°C.

4.2. Inkjet Printing

Inkjet printing is based on the drop-on-demand (DOD) mechanism by which the desired design is transferred directly to the (flexible) substrate. This technology requires no masks compared with the conventional etching technique, which has been commonly used in production, therefore, creating no waste, ensuing in an economical and eco-friendly manufacturing choice. Whereas, the proposed structure, utilizes more ink than [3, 15], but this cost is fully justified for exceptional degree of functionalities offered by the structure. The inkjet printer used in this research is Fujifilm Dimatix DMP2800 which

is a tabletop printer as showed in Figure 5(a). It employs one user fillable piezo-based inkjet print cartridge that has 16 nozzles in a single row with the spacing between two consecutive nozzles is 254 µm, and the substrate is held by vacuum plate. Figure 5(a) also shows the drop watcher view of ink drops of 10 pl in volume are ejecting out of DMC-11610 print cartridge which can be filled upto 1.5 ml.

The antenna structure on Felix Schoeller paper is showed in Figure 5(b) by using Cabot conductive ink having silver solid loading of 19–21 wt%. Furthermore, printing parameters are optimized for all the three paper substrate types using Xerox conductive ink having silver loading of 40 wt%. The optimized jetting voltage realized for both inks is 16–20 V with the velocity of around 5 m/s. The nozzle temperature is kept at room temperature, and the substrate vacuum plate, which is temperature controllable, is maintained at 40°C while printing with either ink. In order to keep the consistency for performing in-depth analysis, each combination is printed with 20 micron drop spacing and print resolution of 1270 dpi. The printer is equipped with Fiducial Camera, which provided the ease of substrate alignment using reference marks, and positioning a print origin or reference point to match substrate placement. Furthermore, it is used for evaluation of features and locations along with inspection and image capture of printed pattern or drops.

Two different sintering processes are evaluated after drying of ink on the substrate, first one is the prevalent method and the other is

Table 2. Annealing parameters for printed antennas.

Substrate	Xerox Ink Nano-AG-120I	Cabot Ink CCI-300	Temperature (°C)	Time (Minutes)
Kodak U-P Photopaper	√	-	140	30
Kodak U-P Photopaper	-	√	150	120
HP Adv. Photopaper	√	-	120	45
HP Adv. Photopaper	-	√	120	120
Felix Schoeller Paper	√	-	110	90
Felix Schoeller Paper	-	√	110	90

"PulseForge Technology" [32]. In the first approach sintering is carried out in the oven with ventilation system at different temperature and time (as mentioned in Table 2), depending upon the combination of ink and substrate, for sufficiently curing, removing the excess solvent and material impurities from the depositions.

The printed samples are also sintered through "PulseForge Technology" by Novacentrix USA, in order to demonstrate sintering and annealing for high-speed roll-to-roll manufacturing often in ambient air (and is capable of up to 1000 feet per minute). This approach enables the use of ultra low temperature and flexible substrates such as paper substrate, which cannot be annealed at high temperatures.

The characterization of the printed structures is carried out under ULTRA-55 Field Emission Scanning Electron Microscope from Carl Zeiss NTS showed in Figures 5(c) & (d). Figures 5(e) & (f) show the SEMs for elaborating the difference between the heating temperatures. At high temperature or by "PulseForge Technology", an almost solid metal conductor is formed so providing a percolation channel for the conduction of electrons throughout the material without obstruction. The sintering process also provides the derived benefit of increasing the bonding of the deposition with the paper substrate.

5. FIELD & CIRCUIT CONCEPTS PARAMETRIC ANALYSIS

A set of precise and thorough methods for evaluation of the reliability parameters and characterization of the proposed fabricated antenna on different paper substrates are implemented. Firstly, five identical structures are printed for each arrangement of ink and paper substrate. Secondly, in this study, an experimental methodology for the characterization of the impedance of the balanced tag antenna is implemented along with the balun structure. The balanced tag antenna is considered as a two-port network and the impedance of the antenna is characterized using network parameters. The antenna is connected to the two ports of a vector network analyzer through a test fixture mentioned in detail in [33]. The influence of the test fixture is deembedded by using a port-extension technique and the antenna impedance can be extracted directly from the measured parameters. Whereas, the broadband balun transforms the unbalanced coaxial mode into balanced two-wire transmission line mode that fed the spiral antenna. The accuracy of the measurements is increased if all errors up to the measuring instrument tip are eliminated [34]. This includes internal VNA errors after the sampler, the cables along with their tips
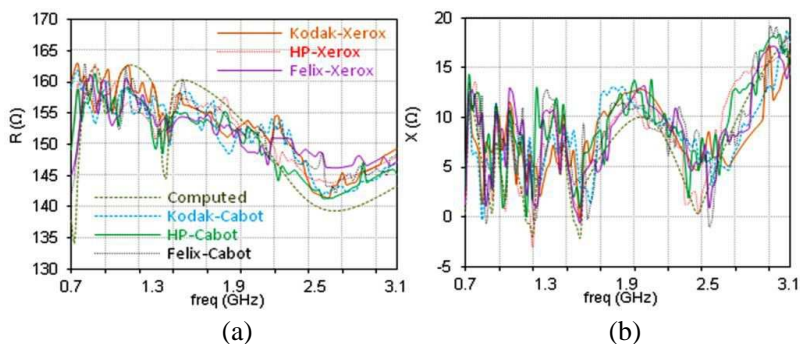
Figure 6. (a) Input resistance variation, (b) input reactance variation.

used to connect to the test structure. The reference plane is shifted to the tips by using the standard calibration methods SOLT (short-open-load-through) for two-ports technique and short-open-load (SOL) for balun structure.

Impedance measurements are carried out using handheld (VNA) vector network analyzer (MS2026B, Anritsu). The impedance graphs are presented in Figure 6 with the largest deviated value at a certain frequency which provides information for worst case analysis, in addition to exploration of performance parameters. This method helps in discovering potential variations that can take place due to the use of paper substrate, which is of critical significance. As showed in Figure 6(a), the measured resistance for the antenna between 1.1–1.4 GHz, fluctuates between 158–144 Ω and from 1.41–3.0 GHz, the variation of resistance is between 146–154 Ω but with much steady manner. However, exceptionally small deviation is pragmatic among the curves of all antennas and this behavior is stable over a much larger frequency range in accordance with published results for spiral structures in [12, 29]. The reactance part of the impedance, as showed in Figure 6(b), follows smaller positive values around 15 Ω with really small variation with frequency. Moreover, relatively constant harmony exists between the computed and measured results. This conforms to both frequency dependent & independent antennas in some extent; however, this behavior of impedance is deliberately achieved because most of the commercially available ASIC till date have also frequency dependence. More importantly, the impedance of the proposed antenna besides easier to match at lower frequencies.

The return loss of the antenna structure is calculated based on the power reflection coefficient. The computed return loss is showed along with measured values of the Xerox ink & Cabot ink printed antennas in Figure 7(a). From Figure 7(a), it is clear
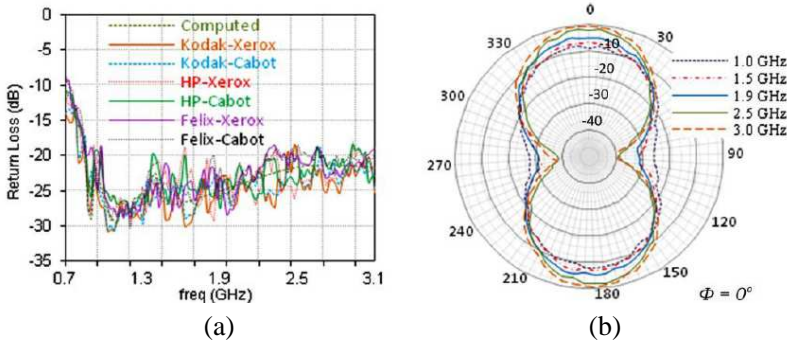
Figure 7. (a) Measured & computed return loss, (b) measured & computed 2D far-field radiation plots.

that the proposed antenna has better return loss and is less than −15 dB throughout the frequency band of interest (and in eloquence with [35, 36]), which is the paramount requirement of antennas for optimal performance. Furthermore, the stable response of paper substrate at higher frequencies, (although with a certain amount of variations but within acceptable values) make it a suitable candidate for broadband antennas. Overall, a good agreement among the computed, Xerox ink printed, and the Cabot ink printed antennas is observed despite the higher metal loss of the silver-based conductive inks.

The radiation pattern is measured inside an anechoic chamber setup that replicates absolute free space [3] (however, half mirror method setup is used in [3]). The spiral antenna under test (AUT) is placed on a positioner assembly, which is set to rotate the antenna in small steps of 5 degrees to obtain a 360° radiation pattern. A continuous-wave (CW) signal from the signal generator excites the AUT. The receiver antenna is connected to the spectrum analyzer (Agilent HP 8562E) and a PC running the test automation software controls the measurement setup. The measured normalized radiation patterns (of antenna printed on Kodak photopaper using Cabot ink) at characteristic frequencies of (1.0, 1.5, 1.9, 2.5) & 3.0 GHz are plotted in Figure 7(b). It is observed that all of the radiation patterns have normal shape and show extreme similarity between computations and measurements, which can also be verified for other frequencies within the antenna bandwidth and are in coherence with previously published results [29]. Additionally, the measured radiation patterns exhibit a slight offset due to the feed line connecting to SMA. It can be depicted from Figure 7(b) that the radiation pattern does not deteriorate in the whole bandwidth from 0.8–3.0 GHz.

6. CONCLUSION

In this paper, it is the first time to propose wideband spiral antennas fabricated on paper substrate for simultaneously implementing a wide range of different modules in addition to, RFID tag. It is noted that adjusting the gap between the adjacent tracks to create the spiral arms leads to a larger number of turns within the same aperture size. All the previously published relevant work in contrast to the proposed approach, is focused on complex techniques, to make such antennas using nonflexible or contaminated substrates, which neither can be implemented with roll-to-roll printing nor suitable for eco-friendly applications. Although the presented research is specific to inkjet printed Archimedean spiral antennas, the same approach can be applied to other antennas made of printed strips, to form modules for "green" electronics.

ACKNOWLEDGMENT

REFERENCES

1. Kim, M., K. Kim, and N. Chong, "RFID based collision-free robot docking in cluttered environment," *Progress In Electromagnetics Research*, Vol. 110, 199–218, 2010.

2. Garcia, J. A., L. Cabria de Juan, R. Marante, L. Rizo, and A. Mediavilla, "An unbiased dual-mode mixing antenna for wireless transponders," *Progress In Electromagnetics Research*, Vol. 102, 1–14, 2010.

3. Amin, Y., Q. Chen, H. Tenhunen, and L. R. Zheng, "Performance-optimized quadrate bowtie RFID antennas for cost-effective and eco-friendly industrial applications," *Progress In Electromagnetics Research*, Vol. 126, 49–64, 2012.

4. Tiang, J.-J., M. T. Islam, N. Misran, and J. S. Mandeep, "Circular microstrip slot antenna for dual-frequency RFID application," *Progress In Electromagnetics Research*, Vol. 120, 499–512, 2011.

5. Meng, Y. S. and Y. H. Lee, "Investigations of foliage effect on

modern wireless communication systems: A review," *Progress In Electromagnetics Research*, Vol. 105, 313–332, 2010.

6. Li, X., J. Liao, Y. Yuan, and D. Yu, "Eye-shaped segmented reader antenna for near-field UHF RFID applications," *Progress In Electromagnetics Research*, Vol. 114, 481–493, 2011.

7. Alejos, A. V., M. G. Sánchez, I. Cuinas, and J. C. G. Valladares, "Sensor area network for active RTLS in RFID tracking applications at 2.4 GHz," *Progress In Electromagnetics Research*, Vol. 110, 43–58, 2010.

8. Jamlos, M. F., A. R. B. Tharek, M. R. B. Kamarudin, P. Saad, O. A. Aziz, and M. A. Shamsudin, "Adaptive beam steering of RLSA antenna with RFID technology," *Progress In Electromagnetics Research*, Vol. 108, 65–80, 2010.

9. Panda, J. R. and R. S. Kshetrimayum, "A printed 2.4 GHz/5.8 GHz dual-band monopole antenna with a protruding stub in the ground plane for WLAN and RFID applications," *Progress In Electromagnetics Research*, Vol. 117, 425–434, 2011.

10. Sim, Z. W., R. Shuttleworth, M. J. Alexander, and B. D. Grieve, "Compact patch antenna design for outdoor RF energy harvesting in wireless sensor networks," *Progress In Electromagnetics Research*, Vol. 105, 273–294, 2010.

11. Jamlos, M. F., A. R. B. Tharek, M. R. B. Kamarudin, P. Saad, M. A. Shamsudin, and A. M. M. Dahlan, "A novel adaptive Wi-Fi system with RFID technology," *Progress In Electromagnetics Research*, Vol. 108, 417–432, 2010.

12. Guraliuc, A. R., R. Caso, P. Nepa, and J. L. Volakis, "Numerical analysis of a wideband thick archimedean spiral antenna," *IEEE Antennas and Wireless Propagation Letters*, Vol. 11, 168–171, 2012.

13. Ramos, A., A. Lazaro, D. Girbau, and R. Villarino, "Time-domain measurement of time-coded UWB chipless RFID tags," *Progress In Electromagnetics Research*, Vol. 116, 313–331, 2011.

14. Chen, A.-X., T.-H. Jiang, Z. D. Chen, and D. Su, "A novel low-profile wideband UHF antenna," *Progress In Electromagnetics Research*, Vol. 121, 75–88, 2011.

15. Amin, Y., Q. Chen, H. Tenhunen, and L. R. Zheng, "Evolutionary versatile printable RFID antennas for "Green" electronics," *Journal of Electromagnetic Waves and Applications*, Vol. 26, Nos. 2–3, 264–273, 2012.

16. Mahmoud, K. R., "Design optimization of a bow-tie antenna for 2.45 GHz RFID readers using a hybrid BSO-NM algorithm,"

Progress In Electromagnetics Research, Vol. 100, 105–117, 2010.

17. Filipovic, D. S. and J. L. Volakis, "Broadband meanderline slot spiral antenna," *2002 IEE Proceedings — Microwaves, Antennas and Propagation*, 98–105, 2002.

18. Zhu, Y.-Z. and J.-D. Xu, "Design of two-arm conical spiral antenna for low elevation angle communication," *Journal of Electromagnetic Waves and Applications*, Vol. 24, Nos. 5–6, 785–794, 2010.

19. Liao, W.-J., S.-H. Chang, and L.-K. Li, "A compact planar multiband antenna for integrated mobile devices," *Progress In Electromagnetics Research*, Vol. 109, 1–16, 2010.

20. Tze-Meng, O., K. G. Tan, and A. W. Reza, "A dual-band omnidirectional microstrip antenna," *Progress In Electromagnetics Research*, Vol. 106, 363–376, 2010.

21. Secmen, M. and A. Hizal, "A dual-polarized wide-band patch antenna for indoor mobile communication applications," *Progress In Electromagnetics Research*, Vol. 100, 189–200, 2010.

22. Ou Yang, J., S. Bo, J. Zhang, and F. Yang, "A low-profile unidirectional cavity-backed log-periodic slot antenna," *Progress In Electromagnetics Research*, Vol. 119, 423–433, 2011.

23. De Cos, M. E., Y. Alvarez Lopez, R. C. Hadarig, and F. Las-Heras, "Flexible uniplanar artificial magnetic conductor," *Progress In Electromagnetics Research*, Vol. 106, 349–462, 2010.

24. Chen, J., G. Fu, G.-D. Wu, and S.-X., Gong, "A novel broadband circularly polarized irregular slot antenna," *Journal of Electromagnetic Waves and Applications*, Vol. 24, Nos. 2–3, 413–421, 2010.

25. Richard, C. J., *Antenna Engineering Handbook*, McGraw-Hill Inc., New York, 1992.

26. Balanis, C. A., *Antenna Theory*, John Wiley and Sons Inc., New Jersey, 2005.

27. Lin, D.-B., I.-T. Tang, and C.-C. Wang, "UHF RFID H-shaped tag antenna using microstrip feed design on metallic objects," *Journal of Electromagnetic Waves and Applications*, Vol. 25, No. 13, 1828–1839, 2011.

28. Hsu, H.-T., F.-Y. Kuo, and C.-H. Chang, "Application of quasi log- periodic antenna for UHF passive RFID tag design featuring constant power transmission coefficient over broadband operation," *Journal of Electromagnetic Waves and Applications*, Vol. 24, Nos. 5–6, 575–586, 2010.

29. Chen, T.-K. and G. H. Huff, "Stripline-fed archimedean spiral

antenna," *IEEE Antennas and Wireless Propagation Letters*, Vol. 10, 346–349, 2011.

30. Huang, Y. and K. Boyle, *Antennas from Theory to Practice*, John Wiley & Sons Ltd., New York, 2008.

31. Da Silveira, F. E. M. and J. A. S. Lima, "Skin effect from extended irreversible thermodynamics perspective," *Journal of Electromagnetic Waves and Applications*, Vol. 24, Nos. 2–3, 151–160, 2010.

32. PulseForge Technology, Available at www.novacentrix.com.

33. Kuo, S.-K., J.-Y. Hsu, and Y.-H. Hung, "Analysis and design of an UHF RFID metal tag using magnetic composite material as substrate," *Progress In Electromagnetics Research B*, Vol. 24, 49–62, 2010.

34. Zhao, W., Y.-J. Zhao, and H.-B. Qin, "Calibration of the three-port VNA using the general 6-term error model," *Journal of Electromagnetic Waves and Applications*, Vol. 24, Nos. 2–3, 319–326, 2010.

35. Schreider, L., X. Begaud, M. Soiron, B. Perpere, and C. Renard, "Broadband Archimedean spiral antenna above a loaded electromagnetic band gap substrate," *IET Microwaves, Antennas & Propagation*, Vol. 1, No. 1, 212–216, 2007.

36. Bell, J. M. and M. F. Iskander, "A low-profile Archimedean spiral antenna using an EBG ground plane," *IEEE Antennas and Wireless Propagation Letters*, Vol. 3, 223–226, 2004.